Large-Scale Control on the Patagonian Climate

R. GARREAUD, P. LOPEZ, M. MINVIELLE, AND M. ROJAS

Department of Geophysics, Universidad de Chile, Santiago, Chile

(Manuscript received 13 December 2011, in final form 10 May 2012)

ABSTRACT

Patagonia, located in southern South America, is a vast and remote region holding a rich variety of past environmental records but a small number of meteorological stations. Precipitation over this region is mostly produced by disturbances embedded in the westerly flow and is strongly modified by the austral Andes. Uplift on the windward side leads to hyperhumid conditions along the Pacific coast and the western slope of the Andes; in contrast, downslope subsidence dries the eastern plains leading to arid, highly evaporative conditions.

The authors investigate the dependence of Patagonia's local climate (precipitation and near-surface air temperature) year-to-year variability on large-scale circulation anomalies using results from a 30-yr-long high-resolution numerical simulation. Variations of the low-level zonal wind account for a large fraction of the rainfall variability at synoptic and interannual time scales. Zonal wind also controls the amplitude of the air temperature annual cycle by changing the intensity of the seasonally varying temperature advection.

The main modes of year-to-year variability of the zonal flow over southern South America are also investigated. Year round there is a dipole between mid- and high latitudes. The node separating wind anomalies of opposite sign migrates through the seasons, leading to a dipole over Patagonia during austral summer and a monopole during winter. Reanalysis data also suggests that westerly flow has mostly decreased over north-central Patagonia during the last four decades, causing a drying trend to the west of the Andes, but a modest increase is exhibited over the southern tip of the continent.

1. Introduction

Patagonia is a large and diverse region in southern South America that extends from about 40°S down to the southern tip the continent (55°S), including Tierra del Fuego and the southernmost section of the Andes cordillera (Fig. 1). Western (Chilean) Patagonia is the narrow (~50–150 km), intricate strip of land from the Pacific coast to the Andean crest that rises to ~1500 m MSL in these latitudes. To the east of the ridge, Argentinean Patagonia features low-lying (100–200 m MSL), steppelike plains extending for several hundred kilometers to the Atlantic Ocean. Situated in the core of the midlatitudes and downstream of the vast southern Pacific, Patagonia faces strong westerlies throughout the year (Garreaud et al. 2009). The baroclinic waves embedded in the main westerly flow are profoundly perturbed by the austral Andes, leading to one of the most dramatic precipitation gradients on earth (e.g., Smith and Evans 2007; Carrasco et al. 2002); see also Fig. 2a. Western Patagonia features a temperate, hyperhumid climate with freezing levels generally above 1 km MSL, a modest seasonal cycle and annual mean precipitation in the 5000–10 000-mm range (Fig. 2, see also Miller 1976). Such high accumulations arise from the orographic enhancement of synoptic-scale precipitation upstream of the mountains (e.g., Roe 2005) and support extensive rainforests and major rivers, numerous glaciers, the northern and southern Patagonia ice fields (NPI and SPI), and the Cordillera Darwin ice field (CDI). The mean precipitation decreases to less than 300 mm yr^{-1} just a few tens of kilometers downstream of the continental divide, leading to a rapid disappearance of vegetation and a rain shadow that extends all the way to the Atlantic coast where mean precipitation only reaches 500–700 mm yr^{-1} (Fig. 2, see also Prohaska 1976; Paruelo et al. 1998; Carrasco et al. 2002). In addition to its aridity, eastern Patagonia features a continental climate, a winter-to-summer temperature

Corresponding author address: Dr. René Garreaud, Departament of Geophysics, Universidad de Chile, Blanco Encalada 2002, Santiago, Chile.
E-mail: rgarreau@dgf.uchile.cl

DOI: 10.1175/JCLI-D-12-00001.1

© 2013 American Meteorological Society

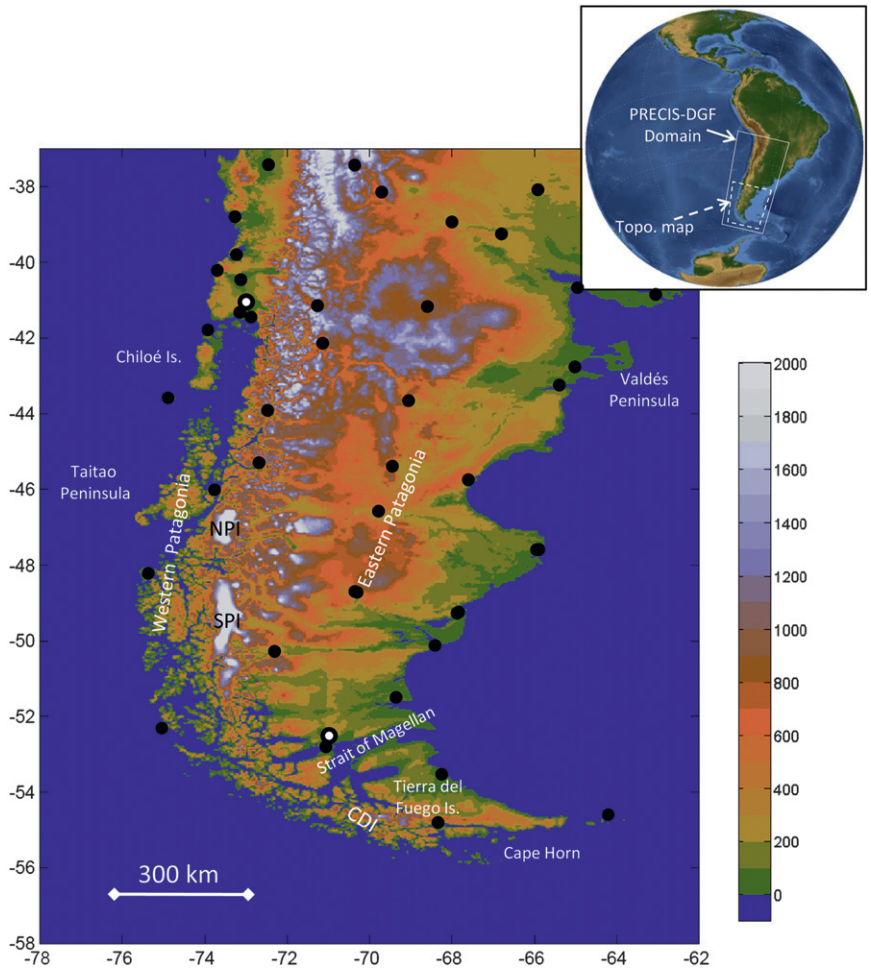


FIG. 1. Topographic map of southern South America (color scale in m MSL) highlighting key features in the Patagonia region. Black circles indicate the location of the meteorological stations used in this work (precipitation and surface air temperature). White circles indicate the location of the regular upper-air (radiosonde) stations: Puerto Montt and Punta Arenas. The upper inset shows the PRECIS-DGF domain used in this work.

amplitude of more than 10°C, and extremely windy, highly evaporative conditions at the surface.

Climate variability in Patagonia is important on its own as a key driver of local changes in the cryosphere and biosphere (e.g., Schneider and Gies 2004; Lara et al. 2005; Rasmussen et al. 2007), but it also can shed light on the functioning of the Southern Hemisphere (SH) extratropical circulation, as South America is the only significant landmass extending southward of 45°S. For instance, the SH annular mode and other hemispheric modes have a significant influence on Patagonia's precipitation and temperature (Gillett et al. 2006; Silvestri and Vera 2003; Garreaud et al. 2009; Quintana and Aceituno 2012), although a causal relationship has not been proposed yet. Furthermore, as reviewed in Villalba et al. (2009), the Patagonia region hosts a rich variety of environmental paleorecords, including ice cores, glaciers, lake and marine sediments, and tree rings, thus offering an excellent opportunity to explore climates of the past in time scales from the late Holocene to the Last Glacial Maximum (LGM) and beyond (e.g., Moreno 2004; Lamy et al. 2010; Blisniuk et al. 2005). There is also mounting evidence of contemporaneous, spatially inhomogeneous trends in precipitation (Quintana and Aceituno 2012; Aravena and Luckman 2009; see section 4b) and subtle but widespread warming (Rosenblüth et al. 1997; Rasmussen et al. 2007) affecting the regional cryosphere. A comprehensive survey in Lopez et al. (2010) found that the majority of Patagonia's glaciers have retreated, some of them quite dramatically, during the second part of the twentieth century and the NPI and SPI have shrunk considerably in the last decades

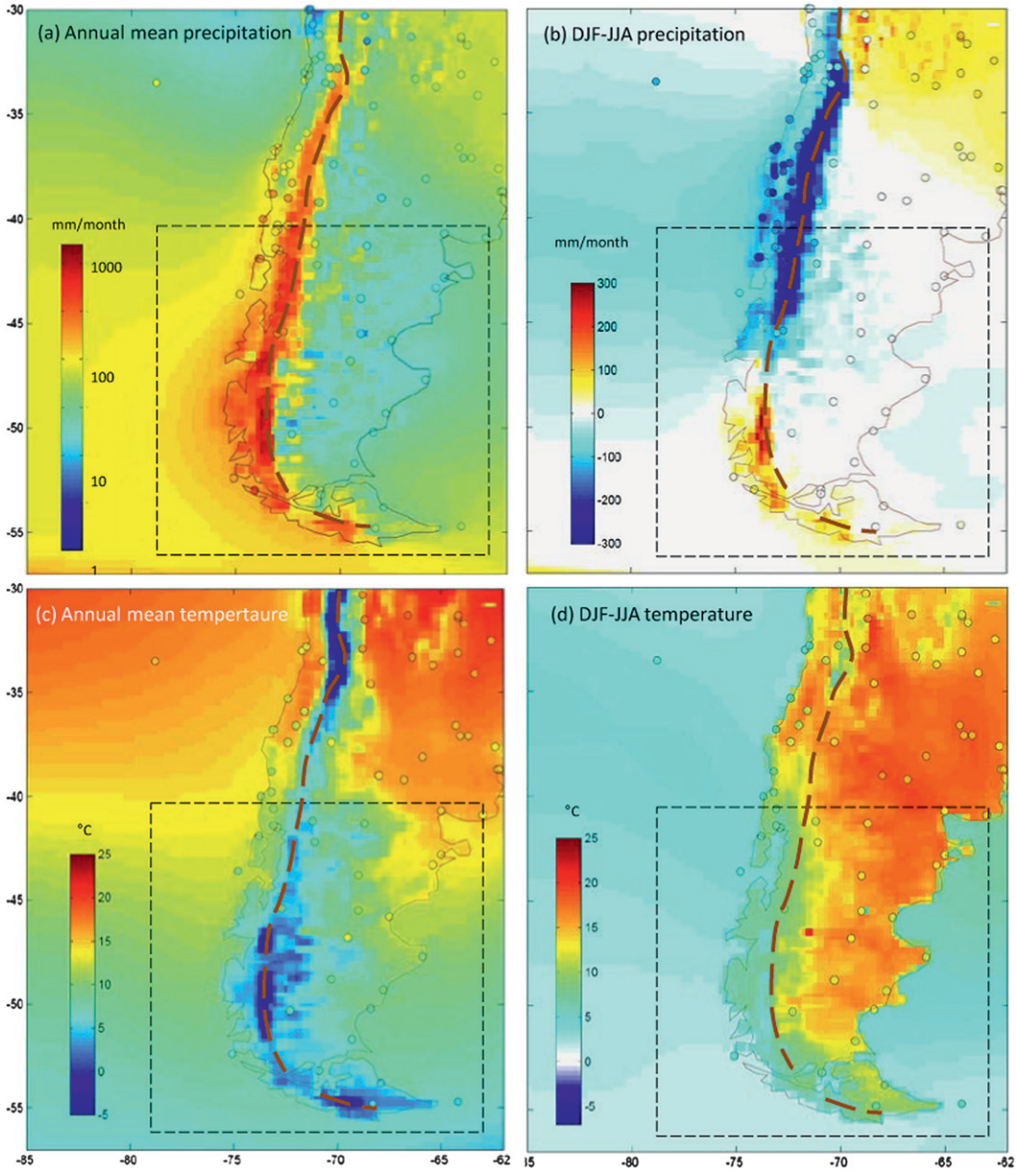


FIG. 2. Comparison of the PRECIS-DGF climatology (shaded) against station observations (circles filled with the same color scale). The model climatology is computed using the period 1978–2001; the station climatology is calculated using all available monthly data during the second half of the twentieth century. Dashed line indicates the ridge of the Andes. (a) Annual mean precipitation; note the logarithmic color scale. (b) Austral summer (DJF) minus winter [June–August (JJA)] mean precipitation. (c) Annual mean near-surface air temperature (1.5 m in the model; approximately 2 m in observations). (d) Austral summer (DJF) minus winter (JJA) mean near-surface air temperature.

(Holmlund and Fuenzalida 1995; Rignot et al. 2003; Aniya 2007). Nevertheless, a few glaciers in the SPI and CDI have advanced or remained stable (Lopez et al. 2010; Möller et al. 2007).

Like many other remote, sparsely populated regions Patagonia lacks a meteorological network with enough spatial density and record length to properly describe climate variability and climate change. With only two regular upper-air stations and less than 20 long-term surface stations (most of them located near the coast, Fig. 1), researchers have pushed the limits of statistical climatology to come up with a regional picture of the climate's mean state and variability or longer trends. To circumvent this problem, here we use output from

the Providing Regional Climates for Impact Studies (PRECIS), a high-resolution, limited-area simulation[1] with lateral boundaries forced by reanalysis data. The reanalysis is able to capture most of the large-scale circulation variability and the regional model performs a dynamical downscaling that is physically consistent with local geography (detailed topography, land use, coastlines, etc.). As documented later, the model shows good agreement with the observations, especially resolving the interannual variability.

The main goal of this work is to quantify and understand the relationship between large-scale circulation (e.g., zonal wind aloft, U) and local climate [precipitation (P) and surface air temperature (SAT)] at interannual time scales, under the premise that variations in the former account for most of the fluctuations in the later. Indeed, using coarse-resolution datasets, Garreaud (2007) found significant correlations between annual mean values of U at 850 hPa and collocated precipitation over the extratropics (particularly strong near the austral Andes), and Rasmussen et al. (2007) investigated the influence of upper-air conditions on the Patagonian ice field using a simple precipitation model forced by reanalysis data. Owing to their nature, large-scale wind anomalies exhibit significant spatial and temporal coherence and are well resolved by atmospheric reanalysis, available for several decades now. In this work we also investigate the main modes of year-to-year variability and contemporaneous trend of the zonal flow over Patagonia, which exhibit important seasonal variations, to infer their impacts on regional P and SAT.

Linking local climate variability with large-scale circulation anomalies has two main applications. First and foremost, it allows a statistical downscaling of large-scale signals to infer, interpret, and extend regional changes in P and SAT, a worthy effort considering the deficiencies in the observational network. Second, it may help to *upscale* local climate signals, assisting paleoclimate studies. Indeed, a few studies have attempted to resolve changes in the Southern Hemisphere westerlies on the basis of paleorecords in Patagonia (e.g., Lamy et al. 2010; Fletcher and Moreno 2012).

The rest of the paper is organized as follows. In section 2 we describe the observational datasets as well as the regional and global climate model used in this work. A customary validation of the regional climate model over southern South America is included in that section. The covariability between zonal flow aloft and precipitation and surface air temperature over Patagonia is documented in section 3. We begin by briefly exploring the relationship at the scale of individual storms, and then address the year-to-year variation using outputs from a regional simulation of the current climate. Once the strong control of free-tropospheric flow on P and SAT is established, we investigate the main modes of the zonal flow interannual variability (section 4a) and trends during the last decades (section 4b), allowing us to infer their counterparts in precipitation over Patagonia. Section 5 provides a summary of our main findings.

2. Dataset

a. Meteorological observations and reanalysis data

In this study we use monthly rainfall and near surface air temperature (nominally at 2 m above ground) records from 31 stations in southern South America (Fig. 1) from 1948 to 2010, obtained from version 2 of the Global Historical Climate Network (GHCN) (Peterson and Vose 1997). This data provides a station-based climatology and wind–precipitation relationship to compare against model results. The record length is variable, but for each station we have at least 10 yr worth of data; missing values were not filled.

The large-scale state of the atmosphere was characterized using two atmospheric reanalysis: the National Centers for Environmental Prediction (NCEP)–National Center for Atmospheric Research (NCAR) reanalysis (NNR) (Kalnay et al. 1996) and the 40-yr European Centre for Medium-Range Weather Forecast Re-Analysis (ERA-40) (Uppala et al. 2005). ERA-40 was also used to force the regional climate model (see below). Both reanalyses are available at a global, regular $2.5° \times 2.5°$ latitude–longitude grid at standard pressure levels. The original time interval is 6 h, from which daily and monthly averages are calculated. The NNR is available from 1948 to 2011 (routinely updated) and the ERA-40 covers the period from mid-1957 to mid-2002. Such record lengths allow their use for studying interannual and interdecadal variability, but trends derived from reanalysis must be used with caution because the number and type of ingested data has varied over time. Indeed, Bromwich and Fogt (2004) report a significant improvement in the skill of NNR and ERA-40 in the high and midlatitudes of the SH after 1978, coincident with the beginning of the satellite-data assimilation.

b. PRECIS-DGF simulations

The Providing Regional Climates for Impact Studies is a regional climate model developed by the Hadley Centre in the United Kingdom (Jones et al. 2004) that is

[1] An alternative dataset would be the recently released Climate Forecast System Reanalysis (CFSR) (Saha et al. 2010) at a horizontal resolution of 0.3° (comparable with PRECIS-DGF).

widely used for studies on climate change (e.g., Marengo et al. 2009). Like any regional model, PRECIS solves the atmospheric governing equations in an area-limited domain forced by lateral, bottom, and top boundary conditions (BC). We performed a continuous 45-yr-long (1958–2001), 25-km grid-spacing resolution simulation (referred to as PRECIS-DGF) over southern South America (Fig. 1) using 6-hourly ERA-40 as lateral BC and observed sea surface temperature [the Hadley Centre Global Sea Ice and Sea Surface Temperature (HadISST) dataset] (Rayner et al. 2003] as bottom BC. Two-dimensional outputs (e.g., near-surface air temperature and precipitation rate) are available every six hours on a regular $0.25° \times 0.25°$ latitude–longitude grid; three-dimensional outputs (e.g., zonal wind and air temperature) have the same horizontal and temporal resolution and were interpolated to standard pressure levels (including 850 and 500 hPa).

Given its configuration, the ability of PRECIS-DGF to simulate the atmospheric mean state and variability is critically dependent on the capacity of ERA-40 to resolve the large-scale circulation over South America and the adjacent oceans, so we decided to restrict our analysis to the period 1978–2001. A detailed evaluation of the PRECIS-DGF modeling system is given in Fuenzalida et al. (2007) and Garreaud and Falvey (2009). [The availability of these independent verifications of the PRECIS-DGF performance over southern South America was an important reason to choose the model output as the primary dataset for the present analysis instead of the recently released Climate Forecast System Reanalysis (CFSR) dataset]. Figures 2a and 2b show the annual mean and seasonal amplitude of the precipitation over southern South America using the PRECIS-DGF results. To facilitate comparison, station-based long-term mean values are superimposed on the simulated field using the same color scale. The model is able to capture the gradual north-to-south increase in precipitation along the Pacific coast and the sharp gradient across the austral Andes. As noted before, there is a lack of surface stations in western Patagonia, but simulated mean accumulations in the 2000–11 000 mm yr^{-1} range are consistent with independent estimates based on river discharge (DGA 1987; Escobar et al. 1992), satellite-derived precipitation offshore (Falvey and Garreaud 2007), and the mass balance over the NPI/SPI (e.g., Rignot et al. 2003). The model, however, overestimates by a factor of ~2 the mean precipitation over high terrain at subtropical latitudes (30°–35°S) where the Andes cordillera exceeds 4000 m MSL. On the other hand, PRECIS-DGF correctly simulates the annual cycle of precipitation (Fig. 2b) characterized by a wintertime maximum at subtropical and midlatitudes and a conspicuous *minimum* to the south of 47°S. Likewise, the annual mean and seasonal amplitude of the surface air temperature are well simulated by the model over Patagonia (Figs. 2c,d).

Since PRECIS-DGF was forced by realistic, time-varying lateral (ERA-40) and bottom (HadISST) boundary conditions, the model also mimics precipitation and temperature variability at daily to interannual time scales. As an example, Fig. 3 shows the observed and simulated annual mean time series of P and SAT in Puerto Montt (northern Patagonia) and Punta Arenas (southern Patagonia). A more complete analysis of the PRECIS-DGF ability to simulate year-to-year precipitation changes in Patagonia is provided by Fuenzalida et al. (2007), who conclude that the PRECIS-DGF simulation realistically represents the interannual variability as well as the annual and seasonal precipitation trend over the 1978–2001 period. In the free troposphere, the PRECIS-DGF simulation closely follows the ERA-40 circulation and properly captures the westerly wind belt at midlatitudes and the upper-level jet stream. In summary, the PRECIS-DGF simulation provides a long (1978–2001), subdaily, high-resolution (0.25°) dataset over southern South America that reproduces the main features of the regional climate, climate variability, and synoptic-scale fluctuations. Because this dataset was created using a dynamical model (instead of interpolating station data), it is also physically consistent and therefore amenable to diagnose the relationship between the wind field aloft and surface conditions.

3. Zonal wind control on precipitation and surface air temperature

a. Storm-scale behavior

Before we describe the year-to-year covariability of precipitation and wind aloft, it is instructive to briefly explore their association at the scale of individual storms. To this effect, Fig. 4 shows the local (point-to-point) correlation map between *daily* averages of precipitation (P) and the 850-hPa wind components (U_{850}, V_{850}) from the PRECIS-DGF simulation, conditioned to presence of precipitation ($P > 1$ mm day^{-1}). The synoptic-scale environment during storms over southern South America typically features a midlatitude trough with its axis just to the west of the Andes and northwesterly flow in the free troposphere (e.g., Barrett et al. 2011). Nevertheless, the association between wind and precipitation widely varies across the domain. Over the South Pacific there is a moderate correlation between precipitation and collocated wind aloft, with $r(P, U_{850}) \sim -r(P, V_{850}) \sim +0.5$, indicative of high precipitation under strong synoptic forcing. Closer to the continent the correlation with the zonal (meridional) flow

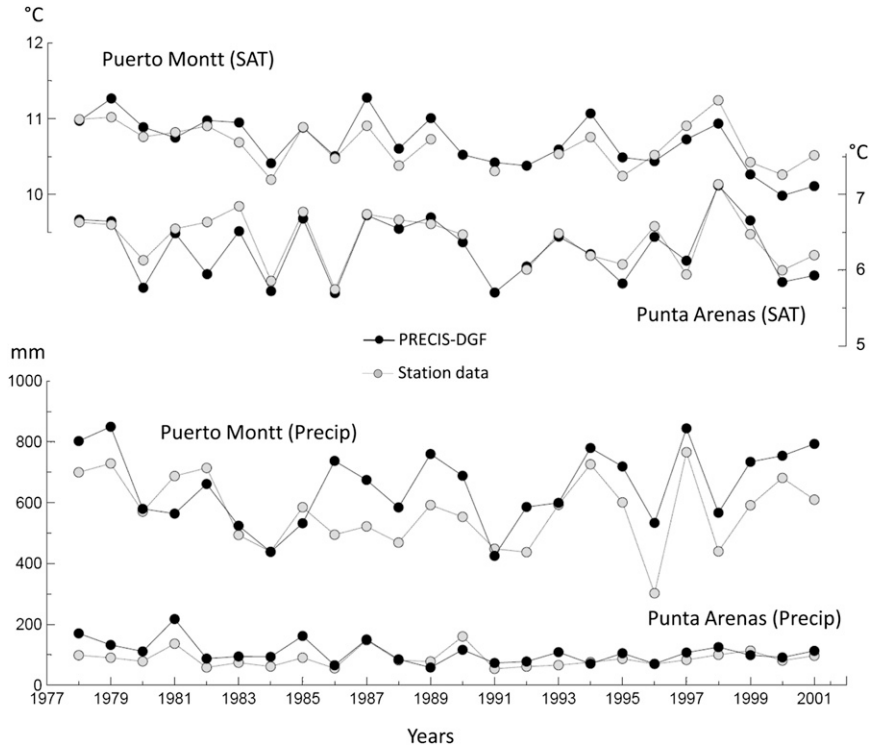


FIG. 3. Time series of observed (gray circles) and PRECIS-DGF (black circles) annual mean near-surface (top) air temperature and (bottom) precipitation in Puerto Montt (northwestern Patagonia; 41.5°S, 72.8°W) and Punta Arenas (southeastern Patagonia; 53.2°S, 70.9°W).

increases (decreases) until reaching the western slope of the Andes where $r(P, U_{850}) \sim +0.7$ and $r(P, V_{850}) \sim -0.3$. The strong dependence of precipitation on zonal flow aloft is remarkably uniform along extratropical Chile and results from the orographic enhancement of precipitation, as midlevel flow normal to the Andes produces upslope flow acting in concert with the synoptic-scale ascent [see Roe (2005) for a review]. These PRECIS results are also consistent with the analysis in Falvey and Garreaud (2007) on the basis of daily rainfall station and radiosonde data in central Chile (32°–36°S).

The orographic enhancement ends sharply at the mountain ridge. Not only does the long-term-mean precipitation decrease by a factor of ~10 from west to east (Fig. 2a), but $r(P, U_{850}) \sim -0.4$ over much of the Argentinean Patagonia (Fig. 4). The few precipitation events in this semiarid region are most often connected with an incoming trough from the South Pacific, the same synoptic pattern that favors rainfall to the west of the Andes. Under these conditions, however, the amount of precipitation tends to be slightly larger in regions under weak westerlies or even easterly flow. Foehn-like windstorms in western Argentina (locally known as *zonda* winds) are well documented around 32°–36°S during frontal episodes in south-central Chile (Seluchi et al. 2003). The same phenomenon is likely to take place farther south, in areas where strong westerlies cross the Andes, resulting in vigorous downslope flow drying the lower troposphere to the east of the ridge and thus locally reducing precipitation in Argentinean Patagonia.

b. Wind–precipitation relationship

Figure 5a shows the local correlation between P and U_{850} using *annual* means from PRECIS-DGF (both fields were detrended). We focus on the precipitation dependence on the zonal flow because this component exhibits much larger year-to-year variation than the meridional component in the SH (e.g., Trenberth 1981). Over southern South America, the interannual $r(P, U_{850})$ map remains similar when considering seasonal means (not shown). To the south of 40°S the correlation pattern exhibits little dependence in the north–south direction with positive values increasing from the South Pacific to a maximum along the Chilean coast and the western slope of the Andes [$r(P, U_{850}) \sim 0.8$], a sharp transition just to the east of the mountain ridge and negative values over the Argentinean Patagonia. Regardless of the latitude, the sign of $r(P, U_{850})$ changes within less than ~100 km from the continental divide (Fig. 5b). Thus, at

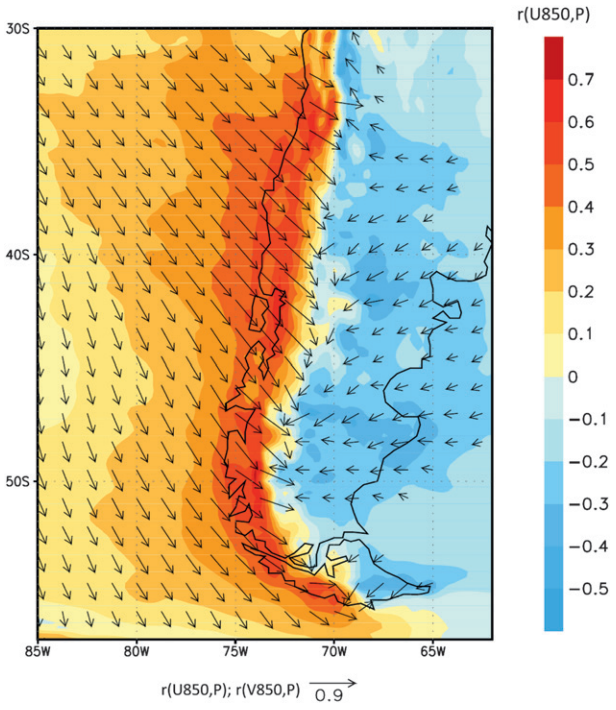


FIG. 4. Local (point-to-point) correlation map between *daily* precipitation (P) and 850-hPa zonal and meridional wind components (U_{850}; V_{850}) using PRECIS-DGF results from 1980–90. At each grid point the correlation was calculated for the sample of days with $P > 1$ mm. Colors indicate the P–U_{850} correlation. Vectors are constructed using $r(P, U_{850})$ and $r(P, V_{850})$ (scale at the bottom) and only shown where absolute value exceeds 0.3.

any zonal transect over Patagonia, a year (or season) with stronger than average midlevel westerly flow features increased precipitation to the west of the Andes and decreased precipitation over the lowlands to the east. The marked west–east precipitation gradient over Patagonia is always present but is slightly less in those years with weaker than average westerly flow aloft.

The scatterplot between monthly mean values of P and U_{850} in two boxes at 50°S further illustrates the strength and nature of their association (Fig. 6). A linear relationship is evident for both sides of the Andes but with significant more dispersion in the dry region to the east. We also constructed the local $r(P, U_z)$ map varying the level z from 1000 to 200 hPa and verified that the overall structure remains similar at different levels although the correlation values are the most significant between 900 and 700 hPa and largest at 850 hPa, approximately the Andean ridge level.

A strong longitude-dependent linear relationship between P and U_{850} is also evident in the interannual $r(P, U_{850})$ map presented by Garreaud (2007) based on NCEP–NCAR reanalysis winds and Climate Prediction Center (CPC) Merged Analysis of Precipitation (CMAP) precipitation (their Fig. 2b), as well as in Fig. 7 constructed using annual mean precipitation at the available stations. The similarity with these observed patterns lends support to our PRECIS-DGF results. Furthermore, the interannual $r(P, U_{850})$ map is quite similar to its daily counterpart (cf. Figs. 4 and 5a), as the correlations at longer times emerge from the aggregated effect of individual storms. The strong covariability between zonal wind aloft and precipitation over western Patagonia seems also to operate within the annual cycle, as the conspicuous wintertime precipitation minimum over the austral Andes (south of 48°S, Fig. 2b) coincides with a seasonal weakening of the westerlies over this region.

c. *Wind–temperature relationship*

We now explore the interannual relationship between the surface air temperature[2] and low-level zonal flow. Over southern South America the annual mean correlations (not shown) are weak and smaller than their precipitation counterparts (Fig. 5a). The temperature–wind relationship, however, exhibits a marked annual cycle and $r(\mathrm{SAT}, U_{850})$ values can be as large as $r(P, U_{850})$ in individual seasons (Fig. 8). Also note that the correlation between seasonal SAT and zonal wind maintains its sign across the Andes, contrasting with the longitude-dependent $r(P, U_{850})$ pattern, and its amplitude decreases toward the tip of the continent.

During summer the correlation is mostly negative, with maximum values along the Chilean coast (~ -0.8) decaying toward the east (Fig. 8a). Negative correlations also dominate during fall, especially along the Chilean coast, but with smaller values. During winter $r(\mathrm{SAT}, U_{850})$ is positive over much of Patagonia with higher values to the east of the Andes (~ 0.8, Fig. 8c). This pattern also appears in spring, but with smaller values. Let us consider a case in which stronger than average westerly flow prevails year round; according to Fig. 8 that would result in a milder winter and a cooler summer, thereby reducing the amplitude of the temperature annual cycle (seasonality) over Patagonia. In contrast, weaker than average westerlies year round result in a colder winter and a warmer summer, thus increasing the temperature seasonality.

[2] The correlations over the ocean are dubious because SAT values there are strongly controlled by the underlying SST, which is prescribed in PRECIS-DGF; in contrast, subsurface temperatures are calculated using a land surface submodel at each time step (including the varying effect of soil temperature and soil moisture) so that SAT over the continent is fully consistent with the atmospheric forcing, including radiative and turbulent heat fluxes as well as temperature advection.

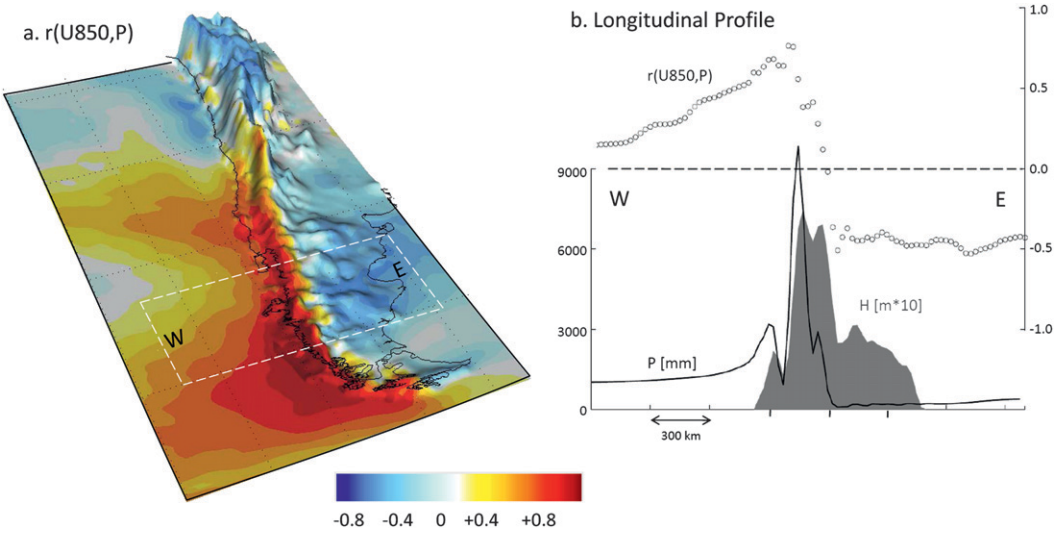


FIG. 5. (a) Local (point to point) correlation between *annual mean* 850-hPa zonal wind and precipitation [$r(U_{850}, P)$] using PRECIS-DGF results from 1978 to 2001. For display purposes the correlation values are shown over the model topography. (b) Longitudinal profile of terrain elevation (shaded area, scale at left), long-term-mean annual precipitation (black line, scale at left in mm yr^{-1}), and the $r(U_{850}, P)$ correlation, averaged between 42° and 52°S. The profiles were constructed every 0.5° of latitude and then composited taken the longitude of highest elevation as a horizontal reference.

The winter-to-summer sign reversal of r(SAT, U_{850}) reflects changes in the low-level energy balance over Patagonia. From spring to summer, insolation tends to warm the land very effectively and, hence, to increase SAT throughout sensible heat fluxes. In contrast, SST over the adjacent South Pacific experience little change and so does the SAT over ocean. Thus, an increase in low-level westerly flow enhances cold air advection over the continent, especially in western Patagonia, leading to a cooler summer season. A similar mechanism explains the mostly positive correlations during winter when an increase in westerly flow enhances advection of warm maritime air over the continent, leading to a milder winter. The key role of the temperature advection in setting r(SAT, U_{850}) underlines the control of the low-level zonal flow on SAT seasonality rather than annual mean SAT values. Indeed, the surface air temperature at any given location in Patagonia is also highly correlated ($r \geq 0.85$, not shown) with the regional-average free tropospheric air temperature (e.g., T_{850}), which is in turn determined by large-scale processes that may occur independent of changes in zonal wind intensity.

4. Zonal wind patterns

The correlation maps presented in the previous section link *local* interannual variations of annual mean precipitation and surface air temperature seasonality with *collocated* 850-hPa zonal flow anomalies. Nevertheless, the zonal wind in the free troposphere does not vary independently from one point to another and organized structures in the large-scale flow will imprint the climate conditions over Patagonia. In this section we explore these structures at different time scales and analyze their impacts on regional P and SAT.

a. Interannual variability

To study the main modes of year-to-year zonal flow variability over southern South America, we applied an EOF analysis to the 850-hPa zonal wind anomalies in the domain 35°–65°S, 90°–60°W (Fig. 9). To isolate the interannual variability we detrended the series by removing a linear fit with time at each grid point. The EOF was performed using the NCEP–NCAR and ECMWF reanalyses (NNR and ERA-40) between 1978 and 2001. The spatial pattern (EOF_1) and loading factor, principle component 1 (PC_1), of the leading mode are quite similar between the two reanalyses, indicative of its robust character. For the sake of brevity we only show results from NNR. The zonal wind field was projected onto the PC to obtain the global signature associated with each mode.

The leading mode accounts for about 40%–50% of the variance in each month and is well separated from the second mode, considering the statistical rule of North et al. (1982). Examination of the monthly EOFs, however, reveals substantial differences in EOF_1 between

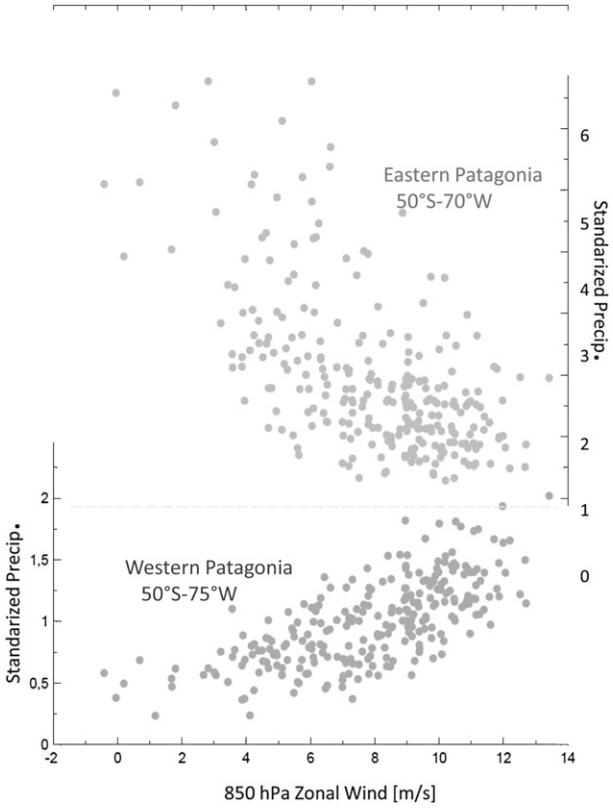


FIG. 6. Scatterplot between monthly precipitation and 850-hPa zonal wind in western and eastern Patagonia. Here we used PRECIS-DGF values from 1978–2001 in two 2° × 2° boxes centered at 50°S, 75°W and 50°S, 70°W. The precipitation values were standardized dividing by their respective long-term means.

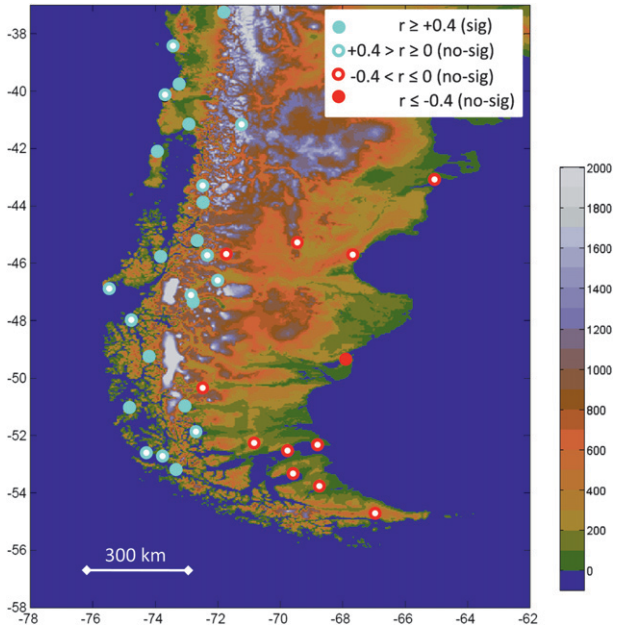


FIG. 7. Correlation coefficient between *annual mean* precipitation and collocated 850-hPa zonal wind (from NNR). Precipitation data from surface observations (at least 15 yr of data). Closed (open) circles indicate correlations significant (not significant) at the 99% confidence level. Red (cyan) circles indicate negative (positive) correlation.

summer and winter months. During austral summer [December–February (DJF)], there are strong, opposite correlations in two zonally elongated bands extending across the whole SH (Fig. 9a). The bands are centered at about 40° and 60°S with the node coincident with the axis of the surface westerly belt. The circumpolar pattern in Fig. 9a is very similar to the Antarctic annular mode (AAO) (e.g., Gong and Wang 1999; Thompson and Wallace 2000; Marshall 2003) and the correlation between PC_1 and the seasonal averaged AAO index reaches +0.7. Thus, we interpret the zonal wind variability over Patagonia during austral summer as part of the hemispheric AAO mode, characterized by a latitudinal vacillation of the tropospheric-deep westerly wind maxima around 50°S.

The EOF_1 during winter–spring also exhibits opposite correlations between mid and high latitudes (Fig. 9b) but the high values are restricted to southern South America and the adjacent Pacific Ocean, and PC_1 is not well correlated with the seasonal AAO index ($r \sim 0.2$). This result[3] is consistent with the less prominent role of the SH annular mode in austral winter documented by Matthewman and Magnusdottir (2012). On the other hand, there are high correlations off the subtropical Chilean coast, where zonal wind anomalies are out of phase with those farther to the south. We also projected the sea level pressure on PC_1 (not shown) to better detect the subtropical forcing of EOF_1. Thus, winter-to-winter zonal wind anomalies over Patagonia are associated with pressure changes in the austral Pacific as well as with fluctuations in the positioning and intensity of the subtropical Pacific anticyclone. When the subtropical anticyclone extends abnormally south, the zonal wind strengthens over southern South America; an anticyclone

[3] Understanding the seasonal change in the leading mode is beyond the scope of this paper. Recall, however, that over the Pacific and during austral summer, there is one single upper-level zonal wind maximum (i.e., subtropical jet merged with the polar front jet) at ~50°S, the same latitude of the surface westerly wind belt. In contrast, during austral winter the subtropical jet migrates to about 30°S and the surface westerlies relax substantially but their maximum remains in the midlatitudes. We speculate that such marked seasonal differences in the background flow may determine the preferred modes of interannual variability in each season, even though the mean field was subtracted before the EOF analysis.

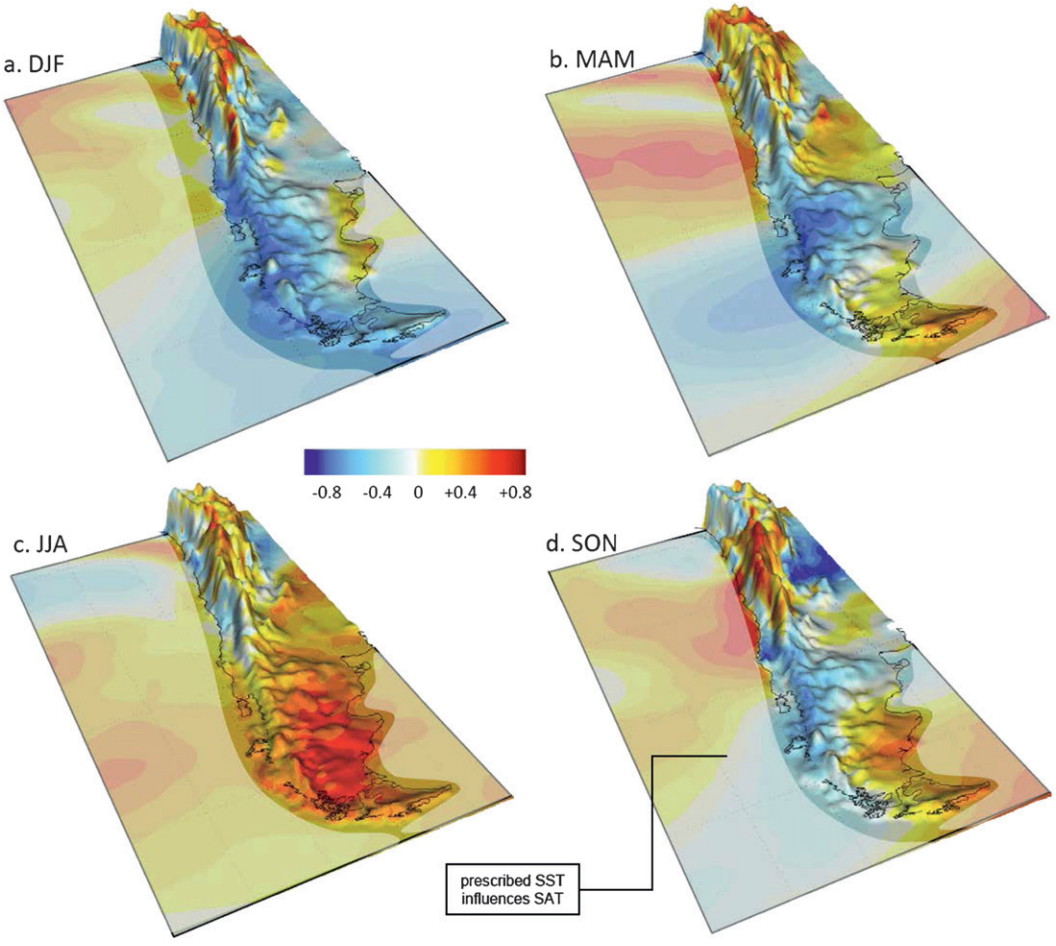


FIG. 8. Local (point to point) correlation between *seasonal mean* 850-hPa zonal wind and surface air temperature, using PRECIS-DGF results from 1978 to 2001. For display purposes the correlation values are displayed over a 3D topography. The $r(U_{850}, \text{SAT})$ values over ocean are slightly masked since SAT there is strongly controlled by the sea surface temperature, which is prescribed in PRECIS-DGF.

more confined to the subtropics is associated with relaxed zonal flow at midlatitudes.

Of particular relevance for our work is the seasonal displacement of the node (the 0-line) in EOF_1 over the continent, most readily seen in a time–latitude section (Fig. 10a). From December to April zonal wind anomalies (enhanced or relaxed westerlies) are out of phase between north-central Patagonia and Tierra del Fuego. In contrast, from May to November the node is located at about 40°S, so the sign of the zonal wind anomalies is uniform over much of southern South America. These results are confirmed by the correlation of U_{850} at each month between one point in central Patagonia and the other at the tip of the continent: moderate positive correlations from June to November and negative correlations the rest of the year (not shown). Considering the P–U_{850} correlations over the western sector of Patagonia, we expect a tendency for a dipole (with its node around 50°S) in summer precipitation variability and a monopole in winter–spring precipitation variability. The temperature interannual variability is less influenced by the seasonal migration of the node in EOF1 since $r(\text{SAT}, U_{850})$ is highest in central Patagonia where the U_{850} anomalies are coherent year round.

The differences in the geographical span of the seasonal EOF_1 are also relevant when attempting to upscale environmental conditions over Patagonia. Precipitation anomalies in summer can be linked with circumpolar anomalies in the low-level (and probably tropospheric-deep) zonal flow at mid and high latitudes, which in turn are well correlated with the hemispheric-scale Antarctic Oscillation (AAO). In contrast, precipitation anomalies in winter can only be linked with low-level westerly wind anomalies in the southeast Pacific and are less correlated with the hemispheric AAO, but they also indicate

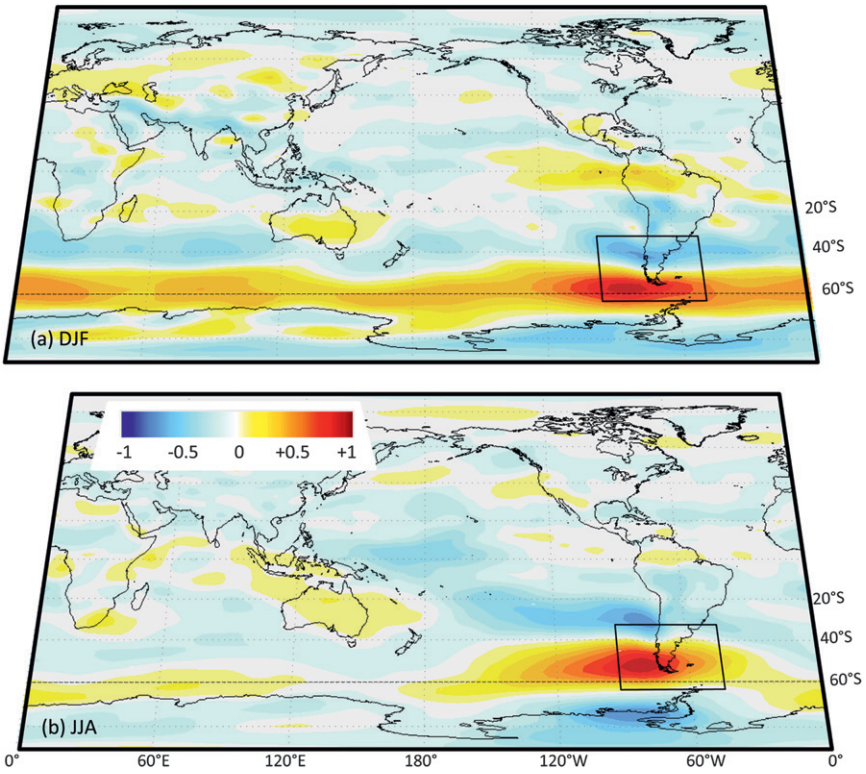


FIG. 9. Leading mode of the 850-hPa zonal (U_{850}) wind interannual variability over southern South America and the adjacent oceans in austral (a) summer and (b) winter using NCEP–NCAR reanalysis data. The EOF analysis was performed for each month in the area outlined by the solid rectangle (35°–65°S, 90°–60°W) and the resulting principal component (time series) was projected on the global U_{850} field. The summer (winter) map was constructed by averaging the DJF (JJA) values at each grid box.

changes in the position and intensity of the subtropical Pacific anticyclone.

b. Contemporaneous trends

Let us now describe the trends in zonal wind over the last few decades when reanalyses are available. Figure 11 shows the linear trend in the annual mean 850-hPa zonal wind using ERA-40 and NNR for the period 1968–2001. Both reanalyses show a band of increasing westerlies over the Southern Ocean around Antarctica (with the largest amplitude in the Atlantic and Indian sectors) and decreasing winds poleward. This dipole in the zonal wind trend is consistent with a tendency of the AAO toward its positive phase (lower pressure at high latitudes), especially in spring–summer, detected in several studies (e.g., Thompson and Solomon 2002; Gillett and Thompson 2003). At midlatitudes there is a tendency toward weaker westerlies, although the signal there is less coherent between the reanalysis and exhibits more dependence on longitude.

To focus on the changes over southern South America, the linear trend for each month was averaged between 75° and 65°W and presented as a time–latitude section in Fig. 10b. Consistent with the hemispheric annual mean trends, decreasing (increasing) westerlies prevails around 45°S (60°S). Both reanalysis indicate a significant reduction of the westerlies over north-central Patagonia throughout the year, but with a larger amplitude during winter and spring. On the other hand, the high-latitude area of increasing westerlies reaches Tierra del Fuego most of the year but leads to significant trends during austral summer only. Such a winter monopole and a summer dipole Pattern in the zonal wind trend is similar to the seasonal march in the leading mode of interannual variability (cf. Fig. 9a). Linear trends of U_{850} derived from radiosonde observations at Puerto Montt (42°S, 73°W) and Punta Arenas (53°S, 71°W) are generally consistent with the previous analysis lending credibility to the reanalysis-based results.

We can use the interannual correlations obtained in section 3b to infer long-term precipitation changes in Patagonia that are congruent with the zonal wind trend, calculated as $\Delta P^* = \beta \Delta U_{850}$, where β is the

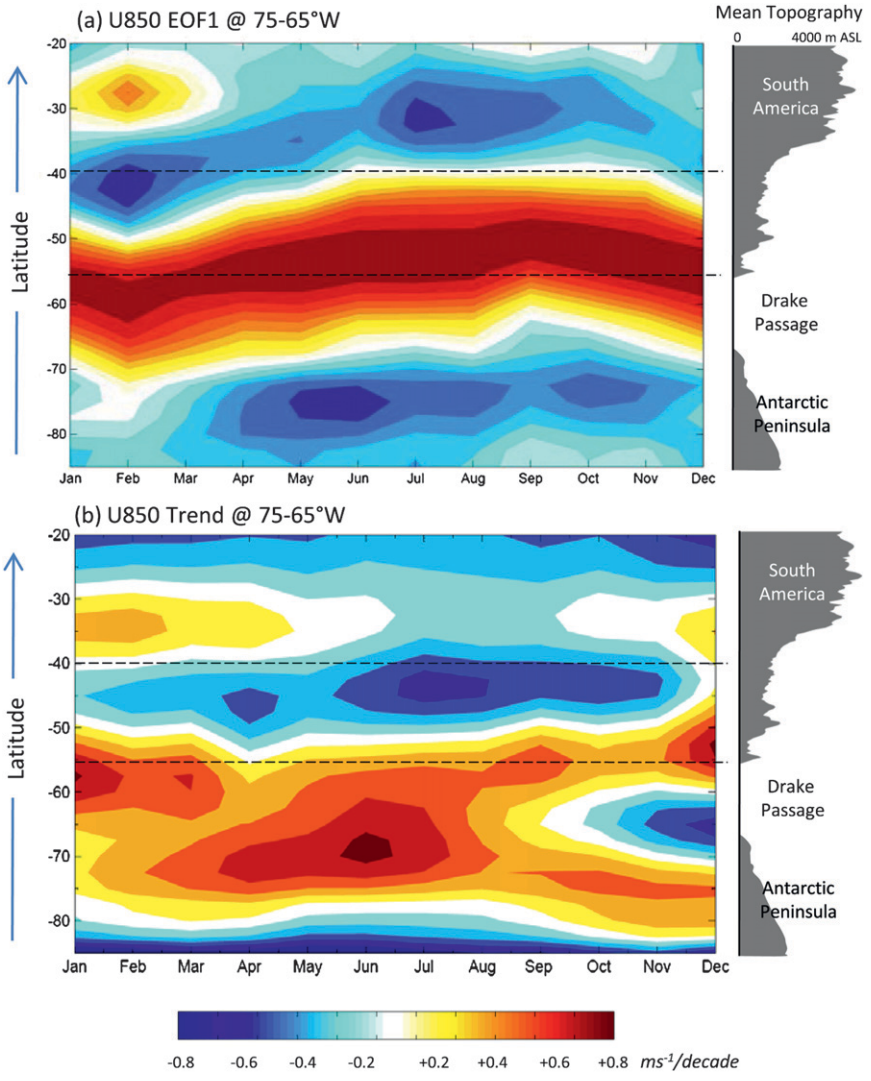


FIG. 10. (a) Latitudinal–seasonal variation of the leading mode of the 850-hPa zonal wind (U_{850}) interannual variability averaged between 75° and 65°W. The EOF analysis was performed for each month in the area outlined in Fig. 10. (b) Linear trends (1968–2001) in U_{850} averaged between 75° and 65°W. The gray area to the right shows the mean topography. Results are based on NCEP–NCAR reanalysis.

slope of the linear fit and ΔU_{850} is the reanalysis mean (average of NNR and ERA-40) zonal wind change between 1968 and 2001 interpolated to each PRECIS-DGF grid box. The slope β has the same pattern as the P–U_{850} correlation coefficient (cf. Fig. 5a); the coarse reanalysis trend ΔU_{850} has little dependence on longitude but it varies more in latitude (cf. Fig. 10b). The results are shown in Fig. 12 for annual accumulations. To the west of the Andean ridge there is a 300–800 mm decade^{-1} decrease in precipitation over north-central Patagonia and ~200 mm decade^{-1} increase to the south of 50°S. Changes in eastern Patagonia are too small and, thus, are not significant. The previous changes per decade represent about ±20% of the long-term annual means. These results are in good agreement with a trend analysis based on station data by Carrasco et al. (2002), Aravena and Luckman (2009), Lopez et al. (2008), and Quintana and Aceituno (2012). Such agreement further indicates that wind-driven changes account for most of the total precipitation changes in western Patagonia. The slight increase in precipitation on the western side of Tierra del Fuego is also compatible with a moderate glacial thickening in the center of the Gran Campo Nevado ice cap (53°S, 73°W) during the period 1984–2000 found by Möller et al. (2007).

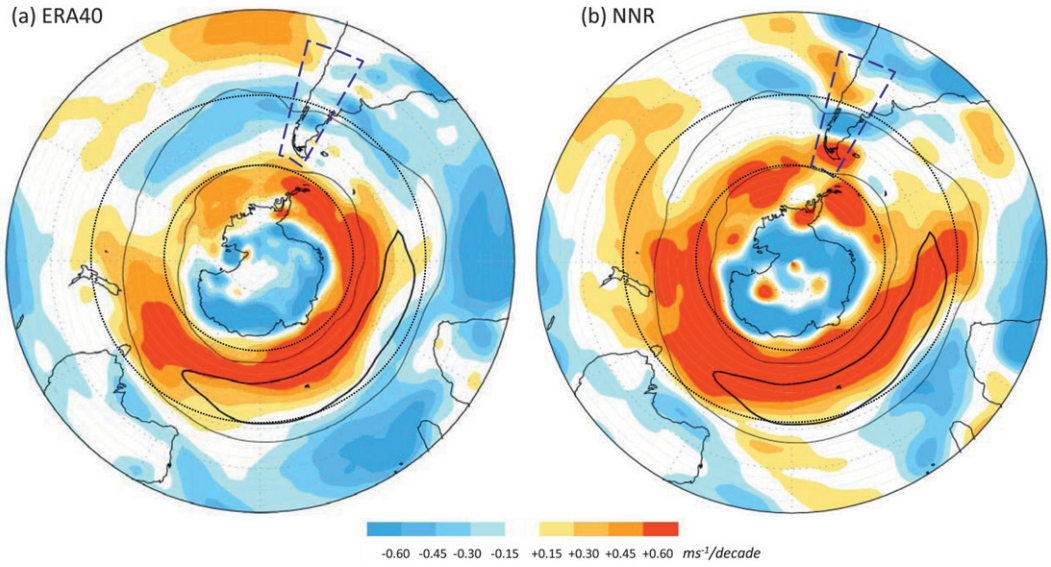


FIG. 11. Linear trends in the *annual mean* zonal wind at 850 hPa (U_{850}) using the (a) ERA-40 and (b) NCEP–NCAR reanalyses. Shading indicates the change between 1968 and 2001 of a linear least squares trend fit calculated at each grid box. The thick (thin) black contour outlined areas where the annual mean U_{850} exceeds 15 m s^{-1} (10 m s^{-1}).

5. Concluding remarks

Interannual variability of precipitation (P) and near-surface air temperature (SAT) over Patagonia is important on its own since it controls changes in the regional cryosphere and biosphere, but it also sheds light on a broader context since southern South America is the only significant landmass in the SH midlatitudes and the region holds a rich variety of past environmental records. Nevertheless, the number of meteorological stations in this vast and diverse region is clearly insufficient to describe its mean climate, interannual variability, and contemporaneous climate change. This problem motivated a central objective of this work in which we try to link local climate variability with large-scale circulation anomalies. The local climate fluctuations are properly

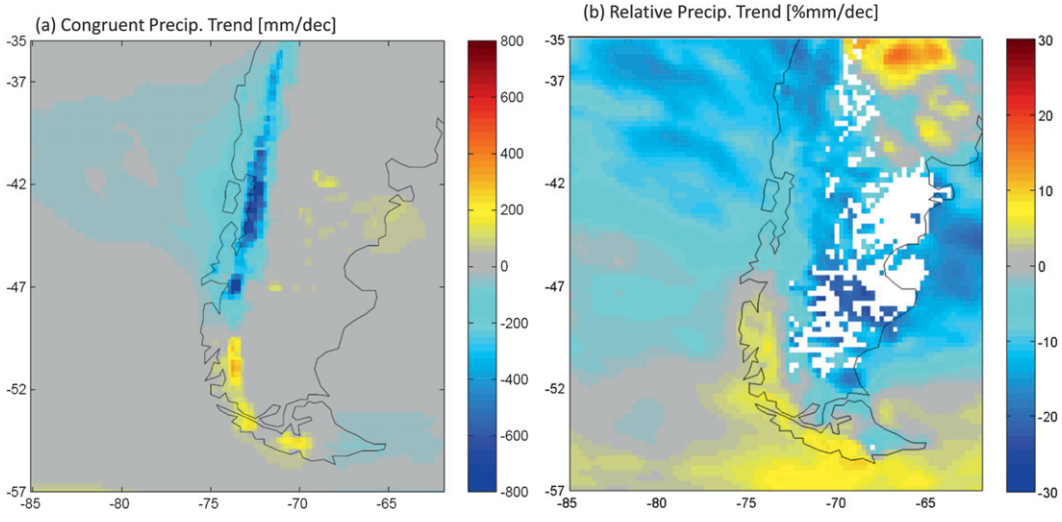


FIG. 12. Annual mean precipitation changes in the period 1968–2001 congruent with the reanalysis (NNR and ERA-40) zonal wind changes (see text for details). (a) Absolute changes in mm decade^{-1}. (b) Absolute changes (mm decade^{-1}) standardized by the long-term-mean annual precipitation (derived from PRECIS-DGF). The relative changes are not shown in areas where the annual mean precipitation is less than 300 mm yr^{-1}.

described by the results of a high-resolution (25-km horizontal grid spacing) regional numerical model (PRECIS) forced by realistic boundary conditions (ERA-40) during the period 1978–2001. The large-scale circulation is described using two reanalysis datasets: ERA-40 and NCEP–NCAR.

By performing a local (point-to-point) linear correlation analysis between the seasonal values of zonal flow at 850 hPa (U_{850}, representative of the low-level circulation) and P and SAT, we reach the following conclusions.

- To the south of 40°S, U_{850} is strongly and positively (negatively) correlated with P to the west (east) of the Andes ridge in all seasons. This result is in line with previous findings and our own analysis based on station data. It indicates that, at any latitude in western (eastern) Patagonia, a season with stronger westerlies will augment (decrease) the local precipitation.
- The P–U_{850} seasonal correlation stems from their association at synoptic scale and is particularly strong because of the mechanical effect of the Andes (windward uplift and leeside subsidence). The P–U_{850} correlation even seems to operate within the annual cycle, as the conspicuous wintertime precipitation minimum over the austral Andes (south of 48°S, Fig. 2b) coincides with a seasonal weakening of the westerlies over this region.
- Over much of Patagonia, U_{850} and SAT are positively correlated during winter but negatively correlated during summer. The sign change of the correlation is borne in the seasonal variation of the low-level air temperature advection from the Pacific Ocean onto the continent. Thus, if stronger (weaker) than normal westerlies prevail year round, that will result in a decreased (increased) amplitude of the local air temperature annual cycle.
- The annual mean surface air temperature depends on other factors as well (e.g., SST and air temperature aloft) so that, in general, it is not possible to diagnose the mean SAT on the basis of U_{850} alone.

The correlation analysis links *local* interannual variability of P and SAT with *collocated* U_{850} anomalies. The latter field, however, exhibits a large-scale organization that was also examined in this work by performing EOF and linear-trend analyses of the zonal flow over southern South America and the adjacent oceans. Our main findings are as follows.

- The year-to-year fluctuations of the seasonal mean flow typically exhibit an out-of-phase behavior between the mid and high latitudes. The node separating wind anomalies of opposite sign migrates through the seasons, leading to a dipole over Patagonia during austral summer and a monopole during winter.
- Coupled with our correlation analysis, the previous result has a major implication in the precipitation variability over western Patagonia: winter-to-winter anomalies tend to be coherent (either positive or negative) over this region, but summer-to-summer anomalies tend to exhibit a dipole with a node around 50°S.
- We also found that precipitation anomalies over Patagonia during summer can be linked with circumpolar anomalous zonal flow at mid and high latitudes and are well correlated with the hemispheric-scale AAO. In contrast, precipitation anomalies in winter can only be linked with low-level westerly wind anomalies in the southeast Pacific and are less correlated with the hemispheric AAO. (Indeed, winter anomalies of the SH flow is dominated by the wavenumber-3 mode rather than by a zonally symmetric AAO pattern).
- Considering the period 1968–2001, both reanalyses exhibit a reduction of the westerlies over north-central Patagonia throughout the year, but with a larger amplitude during winter and spring. On the other hand, the high-latitude area of increasing westerlies reaches Tierra del Fuego most of the year but leads to significant trends during austral summer only.
- Again, coupling the previous finding with the correlation analysis over western Patagonia indicates a 300–800 mm decade^{-1} decrease in precipitation over north-central Patagonia and a 200–300 mm decade^{-1} increase to the south of 50°S. These results are qualitatively in agreement with recent trends estimates based on station data.

Acknowledgments. We acknowledge FONDECYT Grants 1110169 (RG), 1090479 (MR), 1090791 (PL), and 3110120 (MM). We are grateful for constructive comments by two anonymous reviewers and Dr. Dave Rahn.

REFERENCES

Aniya, M., 2007: Glacier variations of Hielo Patagónico Norte, Chile, for 1944/45-2004/05. *Bull. Glaciol. Res.,* **24,** 59–70.

Aravena, J. C., and B. H. Luckman, 2009: Spatio-temporal rainfall patterns in southern South America. *Int. J. Climatol.,* **29,** 2106–2120.

Barrett, B. S., D. B. Krieger, and C. P. Barlow, 2011: Multiday circulation and precipitation climatology during winter rain events of differing intensities in central Chile. *J. Hydrometeor.,* **12,** 1071–1085.

Blisniuk, P. M., L. A. Stern, C. P. Chamberlain, B. Idleman, and P. K. Zeitler, 2005: Climatic and ecologic changes during Miocene surface uplift in the Southern Patagonian Andes. *Earth Planet. Sci. Lett.,* **230,** 125–142.

Bromwich, D. H., and R. L. Fogt, 2004: Strong trends in the skill of the ERA-40 and NCEP–NCAR reanalyses in the high and midlatitudes of the Southern Hemisphere, 1958–2001. *J. Climate,* **17,** 4603–4619.

Carrasco, J., G. Casassa, and A. Rivera, 2002: Meteorological and climatological aspects of the Southern Patagonia Ice Cap. *The Patagonian Icefields: A Unique Natural Laboratory for Environmental and Climate Change Studies,* G. Casassa, F. V. Sepúlveda, and R. M. Sinclair, Eds., Kluwer Academic, 29–41.

DGA, 1987: National water balance. Direccion General de Aguas Tech. Rep., 60 pp.

Escobar, F., F. Vidal, and C. Garin, 1992: Water balance in the Patagonia Icefield. *Glaciological Researches in Patagonia, 1990,* R. Naruse, Ed., Japanese Society of Snow and Ice, 109–119.

Falvey, M., and R. D. Garreaud, 2007: Wintertime precipitation episodes in central Chile: Associated meteorological conditions and orographic influences. *J. Hydrometeor.,* **8,** 171–193.

Fletcher, M. S., and P. I. Moreno, 2012: Have the Southern Westerlies changed in a zonally symmetric manner over the last 14,000 years? A hemisphere-wide take on a controversial problem. *Quat. Int.,* **253,** 32–46.

Fuenzalida, H., P. Aceituno, M. Falvey, R. Garreaud, M. Rojas, and R. Sanchez, 2007: Estudio de variabilidad climática en Chile para el siglo XXI (Study on climate variability for Chile during the 21st century). National Environmental Committee Tech. Rep. [Available online at http://www.dgf.uchile.cl/PRECIS.]

Garreaud, R. D., 2007: Precipitation and circulation covariability in the extratropics. *J. Climate,* **20,** 4789–4797.

——, and M. Falvey, 2009: The coastal winds off western subtropical South America in future climate scenarios. *Int. J. Climatol.,* **29,** 543–554, doi:10.1002/joc.1716.

——, M. Vuille, R. Compagnucci, and J. Marengo, 2009: Present-day South American climate. *Palaeogeogr. Palaeoclimatol. Palaeoecol.,* **281,** 180–195.

Gillett, N. P., and D. W. J. Thompson, 2003: Simulation of recent Southern Hemisphere climate change. *Science,* **302,** 273–275.

——, T. Kell, and P. Jones, 2006: Regional climate impacts of the southern annular mode. *Geophys. Res. Lett.,* **33,** L23704, doi:10.1029/2006GL027721.

Gong, D., and S. Wang, 1999: Definition of Antarctic oscillation index. *Geophys. Res. Lett.,* **26,** 459–462.

Holmlund, P., and H. Fuenzalida, 1995: Anomalous glacier responses to 20th century climatic changes in the Darwin Cordillera, southern Chile. *J. Glaciol.,* **41,** 465–473.

Jones, R. G., M. Noguer, D. C. Hassell, D. Hudson, S. S. Wilson, G. J. Jenkins, and J. F. B. Mitchell, 2004: Generating high resolution climate change scenarios using PRECIS. Met. Office Hadley Center, 40 pp.

Kalnay, E., and Coauthors, 1996: The NCEP/NCAR 40-Year Reanalysis Project. *Bull. Amer. Meteor. Soc.,* **77,** 437–471.

Lamy, F., R. Kilian, H. W. Arz, J. P. Francois, J. Kaiser, M. Prange, and T. Steinke, 2010: Holocene changes in the position and intensity of the southern westerly wind belt. *Nat. Geosci.,* **3,** 695–699, doi:10.1038/ngeo959.

Lara, A., R. Villalba, A. Wolodarsky-Franke, J. C. Aravena, B. H. Luckman, and E. Cuq, 2005: Spatial and temporal variation in *Nothofagus pumilio* growth at tree line along its latitudinal range (35°40′–55°S) in the Chilean Andes. *J. Biogeogr.,* **32,** 879–893.

Lopez, P., K. Najib, J. Carrasco, and G. Casassa, 2008: Analysis of meteorological data from NCEP/NCAR reanalysis, radiosonde data and surface stations, and its relation with glacier behaviour in Patagonia during the last 50 years. *Proc. Fourth EGU Alexander von Humboldt Int. Conf.,* Santiago, Chile, EGU, 73.

——, P. Chevallier, V. Favier, B. Pouyaud, F. Ordenes, and J. Oerlemans, 2010: A regional view of fluctuations in glacier length in southern South America. *Global Planet. Change,* **71,** 85–108.

Marengo, J., R. Jones, L. M. Alves, and M. Valverde, 2009: Future change of temperature and precipitation extremes in South America as derived from the PRECIS regional climate modeling system. *Int. J. Climatol.,* **29,** 2241–2255.

Marshall, G. J., 2003: Trends in the southern annular mode from observations and reanalyses. *J. Climate,* **16,** 4134–4143.

Matthewman, J., and G. Magnusdottir, 2012: Clarifying ambiguity in intraseasonal Southern Hemisphere climate modes during austral winter. *J. Geophys. Res.,* **117,** D03105, doi:10.1029/2011JD016707.

Miller, A., 1976: The climate of Chile. *Climates of Central and South America,* W. Schwerdtgefer, Ed., Vol. 12, *World Survey of Climatology,* Elsevier, 113–145.

Möller, M., C. Schneider, and R. Kilian, 2007: Glacier change and climate forcing in recent decades at Gran Campo Nevado, southernmost Patagonia. *Ann. Glaciol.,* **46,** 136–144.

Moreno, P. I., 2004: Millennial-scale climate variability in northwest Patagonia over the last 15 000 yr. *J. Quat. Sci.,* **19,** 35–47.

North, G. R., T. L. Bell, R. F. Cahalan, and F. J. Moeng, 1982: Sampling errors in the estimation of empirical orthogonal functions. *Mon. Wea. Rev.,* **110,** 699–706.

Paruelo, J. M., A. Beltran, E. Jobbagy, O. E. Sala, and R. A. Golluscio, 1998: The climate of Patagonia: General patterns and controls on biotic processes. *Ecol. Aust.,* **8,** 85–101.

Peterson, T. C., and R. S. Vose, 1997: An overview of the Global Historical Climatology Network Temperature Database. *Bull. Amer. Meteor. Soc.,* **78,** 2837–2849.

Prohaska, F., 1976: The climate of Argentina, Paraguay, and Uruguay. *Climates of Central and South America,* W. Schwerdtgefer, Ed., Vol. 12, *World Survey of Climatology,* Elsevier, 57–69.

Quintana, J., and P. Aceituno, 2012: Changes in the rainfall regime along the extratropical west coast of South America (Chile). *Atmósfera,* **25,** 1–22.

Rasmussen, L., H. Conway, and C. Raymond, 2007: Influence of upper air conditions on the Patagonia icefields. *Global Planet. Change,* **59,** 203–216.

Rayner, N., D. Parker, E. Horton, C. Folland, L. Alexander, D. Rowell, E. Kent, and A. Kaplan, 2003: Global analyses of sea surface temperature, sea ice, and night marine air temperature since the late nineteenth century. *J. Geophys. Res.,* **108,** 4407, doi:10.1029/2002JD002670.

Rignot, E., A. Rivera, and G. Casassa, 2003: Contribution of the Patagonia icefields of South America to sea level rise. *Science,* **302,** 434–437.

Roe, G. H., 2005: Orographic precipitation. *Annu. Rev. Earth Planet. Sci.,* **33,** 645–671.

Rojas, M., and Coauthors, 2009: The last glacial maximum in the Southern Hemisphere in PMIP2 simulations. *Climate Dyn.,* **32,** 525–548, doi:10.1007/s00382-008-0421-7.

Rosenblüth, B., H. Fuenzalida, and P. Aceituno, 1997: Recent temperature variations in southern South America. *Int. J. Climatol.,* **17,** 67–85.

Saha, S., and Coauthors, 2010: The NCEP climate forecast system reanalysis. *Bull. Amer. Meteor. Soc.,* **91,** 1015–1057.

Schneider, C., and D. Gies, 2004: Effects of El Niño–Southern Oscillation on southernmost South America precipitation at 53°S revealed from NCEP–NCAR reanalyses and weather station data. *Int. J. Climatol.,* **24,** 1057–1076.

Seluchi, M. E., F. A. Norte, P. Satyamurty, and S. C. Chou, 2003: Analysis of three situations of the foehn effect over the Andes (zonda wind) using the ETA-CPTEC regional model. *Wea. Forecasting,* **18,** 481–501.

Silvestri, G. E., and C. S. Vera, 2003: Antarctic Oscillation signal on precipitation anomalies over southeastern South America. *Geophys. Res. Lett.,* **30,** 2115, doi:10.1029/2003GL018277.

Smith, R. B., and J. P. Evans, 2007: Orographic precipitation and water vapor fractionation over the southern Andes. *J. Hydrometeor.,* **8,** 3–19.

Thompson, D. W. J., and J. M. Wallace, 2000: Annular modes in the extratropical circulation. Part I: Month-to-month variability. *J. Climate,* **13,** 1000–1016.

——, and S. Solomon, 2002: Interpretation of recent Southern Hemisphere climate change. *Science,* **296,** 895–899.

Trenberth, K. E., 1981: Interannual variability of the Southern Hemisphere 500-mb flow: Regional characteristics. *Mon. Wea. Rev.,* **109,** 127–136.

Uppala, S. M., and Coauthors, 2005: The ERA-40 Re-Analysis. *Quart. J. Roy. Meteor. Soc.,* **131,** 2961–3012.

Villalba, R., M. Grosjeanb, and T. Kiefer, 2009: Long-term multiproxy climate reconstructions and dynamics in South America (LOTRED-SA): State of the art and perspectives. *Palaeogeogr. Palaeoclimatol. Palaeoecol.,* **281,** 175–179.

Copyright of Journal of Climate is the property of American Meteorological Society and its content may not be copied or emailed to multiple sites or posted to a listserv without the copyright holder's express written permission. However, users may print, download, or email articles for individual use.